

Mechanisms of CO₂/H⁺ Sensitivity of Astrocytes

Egor Turovsky,^{1,2} Shefeeq M. Theparambil,³ Vitaliy Kasymov,¹ Joachim W. Deitmer,³ Ana Gutierrez del Arroyo,⁴ Gareth L. Ackland,⁴ Jason J. Corneveaux,⁵ April N. Allen,⁵ Matthew J. Huentelman,⁵ Sergey Kasparov,⁶ Nephtali Marina,¹ and Alexander V. Gourine¹

¹Centre for Cardiovascular and Metabolic Neuroscience, Department of Neuroscience, Physiology and Pharmacology, University College London, London WC1E 6BT, United Kingdom, ²Institute of Cell Biophysics, Russian Academy of Sciences, 142290 Pushchino, Russia, ³Abteilung für Allgemeine Zoologie, Fachbereich Biologie, University of Kaiserslautern, D 67663 Kaiserslautern, Germany, ⁴William Harvey Research Institute, Queen Mary University of London, London EC1M 6BQ, United Kingdom, ⁵Neurogenomics Division, Translational Genomics Research Institute, Phoenix, Arizona 85004, and ⁶School of Physiology & Pharmacology, University of Bristol, Bristol BS8 1TH, United Kingdom

Ventral regions of the medulla oblongata of the brainstem are populated by astrocytes sensitive to physiological changes in P_{CO₂}/[H⁺]. These astrocytes respond to decreases in pH with elevations in intracellular Ca²⁺ and facilitated exocytosis of ATP-containing vesicles. Released ATP propagates Ca²⁺ excitation among neighboring astrocytes and activates neurons of the brainstem respiratory network triggering adaptive increases in breathing. The mechanisms linking increases in extracellular and/or intracellular P_{CO₂}/[H⁺] with Ca²⁺ responses in chemosensitive astrocytes remain unknown. Fluorescent imaging of changes in [Na⁺]_i and/or [Ca²⁺]_i in individual astrocytes was performed in organotypic brainstem slice cultures and acute brainstem slices of adult rats. It was found that astroglial [Ca²⁺]_i responses triggered by decreases in pH are preceded by Na⁺ entry, markedly reduced by inhibition of Na⁺/HCO₃⁻ cotransport (NBC) or Na⁺/Ca²⁺ exchange (NCX), and abolished in Na⁺-free medium or by combined NBC/NCX blockade. Acidification-induced [Ca²⁺]_i responses were also dramatically reduced in brainstem astrocytes of mice deficient in the electrogenic Na⁺/HCO₃⁻ cotransporter NBCe1. Sensitivity of astrocytes to changes in pH was not affected by inhibition of Na⁺/H⁺ exchange or blockade of phospholipase C. These results suggest that in pH-sensitive astrocytes, acidification activates NBCe1, which brings Na⁺ inside the cell. Raising [Na⁺]_i activates NCX to operate in a reverse mode, leading to Ca²⁺ entry followed by activation of downstream signaling pathways. Coupled NBC and NCX activities are, therefore, suggested to be responsible for functional CO₂/H⁺ sensitivity of astrocytes that contribute to homeostatic regulation of brain parenchymal pH and control of breathing.

Key words: acidosis; brainstem; breathing; chemosensitivity; hypercapnia; respiration

Significance Statement

Brainstem astrocytes detect physiological changes in pH, activate neurons of the neighboring respiratory network, and contribute to the development of adaptive respiratory responses to the increases in the level of blood and brain P_{CO₂}/[H⁺]. The mechanisms underlying astroglial pH sensitivity remained unknown and here we show that in brainstem astrocytes acidification activates Na⁺/HCO₃⁻ cotransport, which brings Na⁺ inside the cell. Raising [Na⁺]_i activates the Na⁺/Ca²⁺ exchanger to operate in a reverse mode leading to Ca²⁺ entry. This identifies a plausible mechanism of functional CO₂/H⁺ sensitivity of brainstem astrocytes, which play an important role in homeostatic regulation of brain pH and control of breathing.

Introduction

Astrocytes are known to provide neuronal networks with essential structural and metabolic support. They also control the ionic

environment of the neuropil, support synaptic transmission by supplying neurons with a renewable source of transmitters, and provide a neurovascular coupling interface by mediating cerebrovascular responses to heightened neuronal activity (Haydon

Received April 18, 2016; revised July 21, 2016; accepted Aug. 18, 2016.

Author contributions: E.T., J.W.D., A.G.d.A., M.J.H., N.M., and A.V.G. designed research; E.T., S.M.T., V.K., A.G.d.A., J.J.C., A.N.A., and N.M. performed research; J.W.D. and S.K. contributed unpublished reagents/analytic tools; E.T., S.M.T., V.K., G.L.A., J.J.C., M.J.H., S.K., and A.V.G. analyzed data; A.V.G. wrote the paper.

This work was supported by The Wellcome Trust (A.V.G.), the British Heart Foundation (A.V.G. and N.M.), the Medical Research Council (A.V.G. and S.K.; Ref: 42450), the Russian Foundation for Basic Research Fund (E.T.; Ref: 16-34-00159), and the Deutsche Forschungsgemeinschaft (DE 231/24-1,2). A.V.G. is a Wellcome Trust Senior Research Fellow (Refs: 095064 and 200893). G.L.A. holds a Royal College of Anaesthetists/*British Journal of Anaesthesia*

Basic Science Career Development Award. N.M. is a British Heart Foundation Intermediate Basic Research Science Fellow (Ref: FS/13/5/29927). We thank Professor G. E. Shull (University of Cincinnati) for providing the *NBCe1* knock-out mouse line and M. D. DeBoth and A. L. Siniard for their help with transcriptome data analysis.

The authors declare no competing financial interests.

This article is freely available online through the *JNeurosci* Author Open Choice option.

Correspondence should be addressed to Dr. Alexander V. Gourine, Department of Neuroscience, Physiology and Pharmacology, University College London, Gower Street, London WC1E 6BT, UK. E-mail: a.gourine@ucl.ac.uk.

and Carmignoto, 2006; Magistretti, 2006; Attwell et al., 2010). Recent evidence also suggests that astrocytes modulate the activities of CNS neuronal networks. Astrocytes are not electrically excitable, but display Ca²⁺ excitability and, via release of “gliotransmitters” (such as ATP/adenosine, D-serine, and others), are implicated in the control of neuronal excitability, synaptic transmission, plasticity, and information processing (Volterra and Meldolesi, 2005; Haydon and Carmignoto, 2006; Halassa and Haydon, 2010; Henneberger et al., 2010; Araque et al., 2014).

Brainstem regions adjacent to the ventral surface of the medulla oblongata are populated with pH-sensitive astrocytes, which play an important role in the operation of a fundamental homeostatic mechanism that maintains constant level of arterial and brain P_{CO₂}/[H⁺] by controlling the activity of the brainstem respiratory network (Gourine et al., 2010). Brainstem astrocytes are chemosensitive and functionally specialized to detect physiological changes in P_{CO₂}/[H⁺] (Gourine et al., 2010; Kasymov et al., 2013). They respond to 0.2–0.4 unit decreases in pH with elevations in intracellular Ca²⁺ and increased rate of exocytosis of ATP-containing vesicles (Gourine et al., 2010; Kasymov et al., 2013). Released ATP propagates astroglial Ca²⁺ excitation and activates neurons of the brainstem respiratory networks triggering adaptive increases in breathing (Gourine et al., 2005, 2010). Astroglial dysfunction contributes to the disordered breathing pattern and appears to be responsible for dramatically reduced ventilatory CO₂ sensitivity associated with a prototypical neurological disorder called Rett syndrome caused by mutations of the *methyl CpG binding protein 2 (MeCP2)* gene (Lioy et al., 2011; Garg et al., 2015).

The exact mechanisms linking changes in extracellular and/or intracellular P_{CO₂}/[H⁺] with changes in [Ca²⁺]_i in chemosensitive astrocytes remain unknown. An earlier pharmacological survey that addressed the potential involvement of several putative pH-sensitive targets [including certain K⁺ channels, transient receptor potential channels, and connexin hemichannels] failed to suggest a plausible mechanism of astroglial pH sensitivity (Gourine et al., 2010). Here we tested the hypothesis that acidification-induced Ca²⁺ responses in brainstem astrocytes are dependent on Na⁺/HCO₃⁻ cotransporter (NBC) activity. Expression of high-affinity NBCs (such as the electrogenic Na⁺/HCO₃⁻ cotransporter NBCe1) capable of fast HCO₃⁻ transport and effective cytosolic H⁺ buffering in astrocytes has been demonstrated recently (Theparambil et al., 2014; Theparambil and Deitmer, 2015). NBC activation and facilitated HCO₃⁻ entry may explain intracellular alkalization of astrocytes during hypercapnia observed in some earlier studies (Shrode and Putnam, 1994). We hypothesized that in chemosensitive astrocytes, acidification-induced NBC-mediated HCO₃⁻ and Na⁺ entry triggers increases in [Ca²⁺]_i by activation of the Na⁺/Ca²⁺ exchanger (NCX) to operate in a reverse mode (Rojas et al., 2007).

Materials and Methods

All experiments were performed in accordance with the European Commission Directive 2010/63/EU (European Convention for the Protection of Vertebrate Animals Used for Experimental and Other Scientific Purposes) and the UK Home Office (Scientific Procedures) Act (1986) with project approval from the Institutional Animal Care and Use Committee.

DOI:10.1523/JNEUROSCI.1281-16.2016

Copyright © 2016 Turovsky et al.

This is an Open Access article distributed under the terms of the Creative Commons Attribution License Creative Commons Attribution 4.0 International, which permits unrestricted use, distribution and reproduction in any medium provided that the original work is properly attributed.

Experimental models

Organotypic brain slices. Rat pups [postnatal day (P) 8–P10 of either sex] were killed by halothane overdose. Brainstems were rapidly removed and bathed in ice-cold HBSS without Ca²⁺ with added 20 mM glucose (total 25.6 mM), 10 mM MgCl₂, 1 mM HEPES, 1 mM kynurenic acid, 0.005% phenol red, 100 U ml⁻¹ penicillin, and 0.1 mg ml⁻¹ streptomycin. The medulla was isolated and a sequence of transverse slices (250 μm) was cut. Slices were inspected under a low-magnification dissecting microscope and 2–3 brainstem sections containing the facial nucleus (anatomical landmark for the chemosensitive region) were plated on Millicell-CM organotypic culture membrane inserts. Slices were cultured in medium containing 50% Optimum-1, 25% fetal bovine serum (FBS), 21.5% HBSS, 25 mM glucose, 100 U ml⁻¹ penicillin, and 0.1 mg ml⁻¹ streptomycin. After 3 d, the plating medium was removed and DMEM medium containing 10% FBS, 2 mM L-glutamine, 100 U ml⁻¹ penicillin, and 0.1 mg ml⁻¹ streptomycin was added and subsequently replaced twice a week. In some of the experiments, the astrocytes were targeted to express the (genetically encoded) Ca²⁺ indicator *Case12* using an adenoviral vector (AVV) under the control of an enhanced glial fibrillary acidic protein (GFAP) promoter, as described previously (Guo et al., 2010). AVV-sGFAP-*Case12* was added to the medium at the time of slice culture preparation at 5 × 10⁸–5 × 10¹⁰ transducing units ml⁻¹. Experiments were performed after 7–10 d of incubation.

Acute brain slices. Astrocytes that reside at and near the ventral surface of the brainstem were targeted to express Ca²⁺ indicator *Case12* following stereotaxic microinjections of AVV-sGFAP-*Case12*. Young male Sprague Dawley rats (100–150 g) were anesthetized with ketamine (60 mg kg⁻¹, i.m.) and medetomidine (250 μg kg⁻¹, i.m.) and placed in a stereotaxic frame. Adequate depth of surgical anesthesia was confirmed by the absence of a withdrawal response to a paw pinch. Two microinjections per side of AVV-sGFAP-*Case12* (1 μl each) were delivered into the ventral regions of the medulla oblongata using the following coordinates from bregma: 11 and 12 mm caudal, 1.8 mm lateral, and 8.5–8.8 mm ventral. Anesthesia was reversed with atipamezole (1 mg kg⁻¹, i.m.). For postoperative analgesia, rats received buprenorphine (0.05 mg kg⁻¹ d⁻¹, s.c.) for 3 d. After 7–10 d, the rats were terminally anesthetized with halothane overdose. Brains were removed and placed in ice-cold artificial CSF (aCSF) containing 124 mM NaCl, 26 mM NaHCO₃, 3 mM KCl, 2 mM CaCl₂, 1.25 mM NaH₂PO₄, 1 mM MgSO₄, and 10 mM glucose saturated with 95% O₂/5% CO₂, pH 7.4, with an addition of 9 mM Mg²⁺. Horizontal brainstem slices containing the ventral medullary surface (thickness, ~400 μm) were cut using a vibratome and then were left to recover at room temperature for 1 h in a standard aCSF saturated with 95% O₂/5% CO₂.

Cell culture. Primary astroglial cell cultures were prepared from the cortical and brainstem tissue of rat pups (P2–P3 of either sex) as well as the brainstems of wild-type (C57BL/6) and *NBCe1* knock-out mouse pups (P1–P4 of either sex) as described previously (Kasymov et al., 2013). The animals were killed by isoflurane overdose (rats) or rapid decapitation (mice), the brains were removed, and the ventral regions of the medulla oblongata were dissected out. Brainstem tissue cuts from 2–3 animals were used for each cell culture preparation. After isolation, the cells were plated on poly-D-lysine-coated glass coverslips and maintained at 37°C in a humidified atmosphere of 5% CO₂ and 95% air for a ≥10 d before the experiments. Cultured rat astrocytes were transduced to express fluorescent proteins *Case12* (cyclically permuted green fluorescent protein) or DsRed using adenoviral vectors AVV-sGFAP-*Case12* and AVV-sGFAP-DsRed (5 × 10⁸–5 × 10¹⁰ transducing units ml⁻¹).

Imaging

Optical recordings were performed using Olympus FV1000 confocal microscope or an inverted epifluorescence Olympus microscope equipped with a cooled CCD camera (Retiga, QImaging), as described previously (Angelova et al., 2015; Turovsky et al., 2015). [Ca²⁺]_i responses of individual astrocytes were visualized by recording changes in fluorescence of *Case12* (Gourine et al., 2010; Guo et al., 2010) or conventional Ca²⁺ indicators Fura-2 (Invitrogen) and Fluo-4 (Invitrogen). In the experiments using conventional Ca²⁺ indicators, chemosensitive brainstem

astrocytes were identified by robust Ca²⁺ responses to acidification and lack of Ca²⁺ response to KCl (30 mM) application at the end of the recordings, as described previously (Turovsky et al., 2015). Recordings of acidification-induced [Ca²⁺]_i responses in astrocytes transduced to express *Case12* were performed both in organotypic and acute brainstem slices. For imaging, a section of the membrane with an organotypic slice or an acute slice was placed on an elevated grid in a flow chamber (volume, 2 ml). Recordings were made at 35–37°C in aCSF. The rate of perfusion was 4 ml min⁻¹. Images were obtained using a 40× water-immersion objective. The 488 nm argon laser line was used to excite *Case12* fluorescence, which was measured using a 505–550 nm bandpass filter. Illumination intensity was kept to a minimum (at 0.5–0.7% of laser output).

For simultaneous recordings of changes in [Ca²⁺]_i and [Na⁺]_i, organotypic brainstem slices were loaded with Fura-2 (5 μM; 40 min incubation; 37°C) and Sodium Green (10 μM, Invitrogen; 40 min incubation; 37°C) with the addition of pluronic F-127 (0.005%). After incubation with the dyes, slices were washed three times before the experiment. Changes in [Ca²⁺]_i and [Na⁺]_i were monitored in individual cells using an inverted Olympus microscope with a 20× oil-immersion objective. Excitation light provided by a xenon arc lamp was passing sequentially through a monochromator at 340, 380, and 490 nm (Cairn Research); emitted fluorescence at 515 nm (Fura-2) and 530 nm (Sodium Green) was registered. All test drugs were applied 5–20 min before the experimental challenge.

In a separate experiment, changes in absolute [Na⁺]_i in brainstem astrocytes were estimated following calibration of the Sodium Green signal. Organotypic brainstem slices were perfused with aCSF containing gramicidin D (3 μM), monensin (10 μM), and ouabain (100 μM) to equilibrate Na⁺ across the cell membrane. Changes in Sodium Green fluorescence in response to increasing [Na⁺] (0–100 mM) in the media were recorded and plotted as a function of [Na⁺] to create the calibration curve.

To record [Ca²⁺]_i in cultured brainstem astrocytes of wild-type and NBCe1-deficient mice, the cells were loaded with Fluo-4 (5 μM; 15 min incubation; 20–22°C). Changes in [Ca²⁺]_i were monitored using a confocal laser scanning microscope (LSM-700) with a 40× water-immersion objective. The 488 nm laser light was used to excite Fluo-4 fluorescence and emitted fluorescence was registered using a short-pass emission filter (SP 640).

Drugs

S0859 (10–30 μM; Sanofi-Aventis; Ch'en et al., 2008) and 4,4'-diisothiocyanato-2,2'-stilbenedisulfonic acid (DIDS; 100 μM; Tocris Bioscience) were used to inhibit Na⁺/HCO₃⁻ cotransport. SN-6 (10 μM; Tocris Bioscience) was used to interfere with NCX. Cariporide (10 μM; Tocris Bioscience) and amiloride (0.5 mM; Tocris Bioscience) were used to block Na⁺/H⁺ exchange (NHE). Phospholipase C was inhibited by application of U73122 (10 μM; Tocris Bioscience).

Isolation and purification of astrocytes

Young adult male rats (~100 g) and rat pups (P3 of either sex) were used to isolate cortical and brainstem astrocytes. For all the conditions (brain area/developmental stage), one biological replicate consisted of pooled cells from the cortices and the brainstems of 3–4 animals. The animals were humanely killed by isoflurane overdose and the brains were isolated. The cortex and the brainstem were dissected out and the meninges were removed. The tissue was enzymatically dissociated to make a suspension of individual cells as described previously (Zhang et al., 2014).

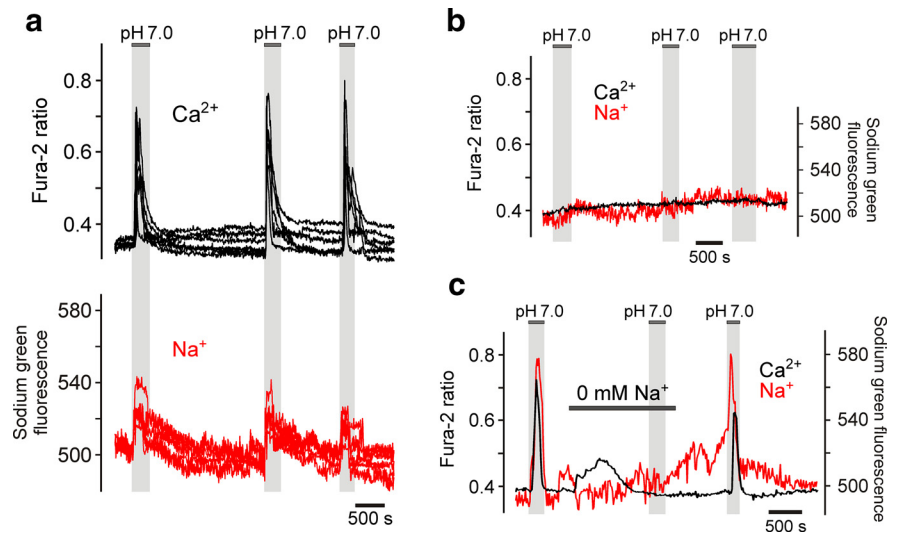


Figure 1. Chemosensory [Ca²⁺]_i responses in brainstem astrocytes are accompanied by Na⁺ entry. **a**, Representative example of [Ca²⁺]_i and [Na⁺]_i responses to CO₂-induced acidification in astrocytes residing near the ventral surface of the medulla oblongata. Traces depict responses of six individual astrocytes in an organotypic brainstem slice preparation. **b**, Lack of Ca²⁺ and Na⁺ responses in astrocytes located in the dorsal aspect of the medulla oblongata. Averaged traces of [Ca²⁺]_i and [Na⁺]_i changes in 19 astrocytes recorded in an organotypic brainstem slice preparation are shown. **c**, Acidification-induced [Ca²⁺]_i responses in chemosensitive astrocytes are reversibly blocked by removal of extracellular Na⁺. Note that low-amplitude lasting increases in [Ca²⁺]_i, which follow introduction of Na⁺-free medium, are likely to be due to the reversal of NCX. Averaged traces of [Ca²⁺]_i and [Na⁺]_i changes in 10 astrocytes recorded in an organotypic brainstem slice are shown.

Briefly, the tissue was incubated at 37°C for 40 min in 20 ml of HBSS containing 0.1% trypsin. After trypsin treatment, the tissue was washed three times with 10 ml of ice-cold HBSS containing FBS (10%) and trypsin inhibitor (1.0 mg ml⁻¹) and then mechanically dissociated by gentle sequential trituration using a 5 ml pipette. Samples were then diluted 10-fold, washed in HBSS, and passed through a 45 μm Nitex mesh to remove undissociated cell clumps before resuspension in 500 μl of PBS containing 0.5% BSA, 2 mM EDTA with the addition of 50 μl of myelin removal beads (Miltenyi Biotec). After 20 min of incubation at 4°C, cells were washed in PBS containing 2 mM EDTA and centrifuged for 10 min (1200 rpm). The cell pellet was resuspended in 500 μl of buffer and applied to a MACS column (Miltenyi Biotec). Magnetic labeled myelin was retained within the column. The second (positive) magnetic separation was then performed using astrocyte-specific anti-GLAST (anti-glutamate/aspartate transporter; ACSA-1) antibodies conjugated to the magnetic beads (Miltenyi Biotec). Anti-O4 selection using magnetic microbeads (Miltenyi Biotec) to separate O4+ immature oligodendrocytes from cell suspensions was also performed to remove ACSA-1-positive astrocytes contaminated by oligodendrocytes. Cell purity was assessed by anti-GLAST (ACSA-1) phycoerythrin antibody (Miltenyi Biotec) using flow cytometry (CyanADP Cytometer, Beckman Coulter). FACS analysis confirmed >95% purity of isolated astrocytes. Purified cells were harvested by centrifugation at 2000 × g for 5 min. The cell pellet was then used for RNA extraction.

Separately, astrocytes in cortical and brainstem cultures transduced with AVV-sGFAP-*Case12* or AVV-sGFAP-DsRed were identified by green or red fluorescence and individually collected using patch pipettes (tip, ~5 μm) made of borosilicate glass. One biological replicate consisted of 20–25 pooled cells from 3–4 cultures; two samples from each brain area were analyzed.

RNA sequencing, read mapping, and expression level estimation

Total RNA was isolated using the RNeasy Plus Micro Kit (Qiagen) following the manufacturer's protocol and RNA quality was assessed using the RNA 6000 Pico Kit on a 2100 Bioanalyzer (Agilent Technologies). Samples containing 100 ng of total RNA were quantified via Nanodrop (Thermo Fisher Scientific) and used to prepare cDNA using the Ovation RNA-seq System v2 following the manufacturer's protocols (Nugen).

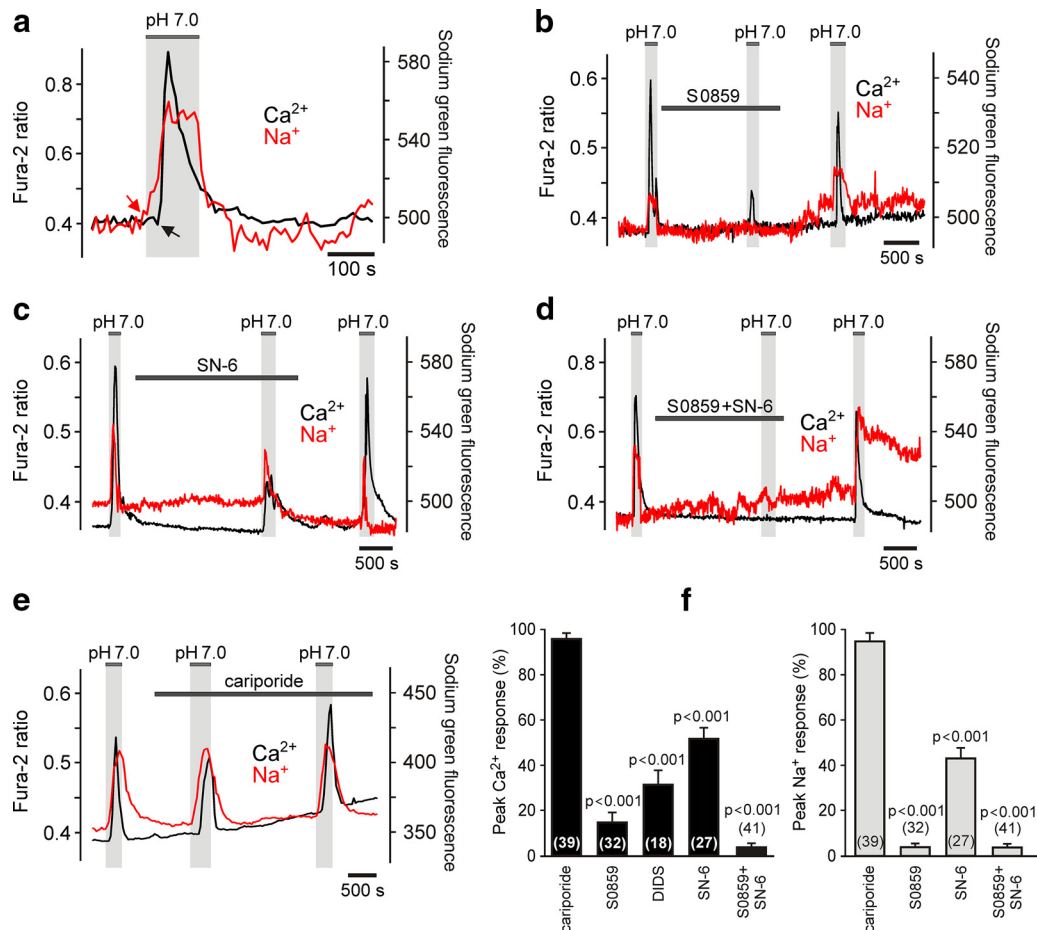


Figure 2. Facilitated Na⁺/HCO₃⁻ cotransport and NCX reversal underlie chemosensory [Ca²⁺]_i responses in brainstem astrocytes. **a**, Expanded representative recording illustrating time course of acidification-induced [Ca²⁺]_i and [Na⁺]_i changes in an individual pH-sensitive astrocyte. CO₂-induced acidification triggers Na⁺ entry, which precedes Ca²⁺ response. **b**, Representative recording illustrating the effect of NBC blocker S0859 (10 μM) on [Ca²⁺]_i and [Na⁺]_i responses of brainstem astrocytes induced by acidification. Averaged traces of [Ca²⁺]_i and [Na⁺]_i changes in 12 astrocytes recorded in an organotypic brainstem slice preparation are shown. **c**, Representative recording illustrating the effect of NCX inhibitor SN-6 (10 μM) on CO₂-induced [Ca²⁺]_i and [Na⁺]_i responses in brainstem astrocytes. Averaged traces of [Ca²⁺]_i and [Na⁺]_i changes in 17 astrocytes recorded in an organotypic brainstem slice are shown. **d**, Representative recording illustrating the effect of combined NBC/NCX blockade [S0859 (10 μM)/SN-6 (10 μM)] on acidification-induced [Ca²⁺]_i and [Na⁺]_i responses in brainstem astrocytes. Averaged traces of [Ca²⁺]_i and [Na⁺]_i changes in 18 astrocytes recorded in an organotypic brainstem slice preparation are shown. **e**, Lack of an effect of NHE inhibitor cariporide (10 μM) on CO₂-induced [Ca²⁺]_i and [Na⁺]_i responses in astrocytes. Averaged traces of [Ca²⁺]_i and [Na⁺]_i changes in 16 astrocytes recorded in an organotypic brainstem slice are shown. **f**, Summary data (expressed as the percentage of the initial response) of the pharmacology of acidification-induced Na⁺ and Ca²⁺ responses in astrocytes recorded in organotypic brainstem slices.

The cDNA was then sonically fragmented with a Covaris S2 system (Covaris) to an average size of 400 bp. Sequencing-ready libraries were prepared using the Truseq DNA Sample Prep Kit (Illumina). Final PCR-enriched fragments were quantified by qPCR using Kapa's Library Quantification Kit (Kapa Biosystems) on the 7900HT (Applied Biosystems). Samples were then pooled before 100 bp paired-end sequencing on two lanes of a HiSeq 2000 (Illumina). Fastq conversion and demultiplexing was conducted with Casava 1.8.2 (Illumina). Reads were aligned to the rat reference genome RGSC3.4.64 with TopHat 1.3.3. Cufflinks v1.0.2 was used to assemble and quantitate the transcriptome of each sample. A union set of transcripts in all samples was generated with Cuffcompare, and differential expression was assessed with Cuffdiff. Expression level is reported as fragments per kilobase of transcript sequence per million mapped fragments values.

Data analysis

Built-in analysis software tools (Olympus or Andor) were used to analyze the results of the imaging experiments. Differences between the experimental groups/treatments were tested for statistical significance by one-way or two-way ANOVA followed by the *post hoc* Tukey–Kramer test, Student's paired *t* test, or Student's unpaired *t* test, as appropriate (NCSS 2007). Data are reported as mean ± SEM. Differences with *p* < 0.05 were considered to be significant.

Results

Brainstem regions adjacent to the ventral surface of the medulla oblongata are populated by astrocytes that respond to acidification (decreases in pH from 7.4 to 7.0 induced by an increase in P_{CO2} from 40 to ~80 mmHg in aCSF containing 26 mM HCO₃⁻) with elevations in intracellular [Ca²⁺]_i (Figs. 1–4). Robust Ca²⁺ responses to decreases in pH are observed both in cultured organotypic brainstem slices (Fig. 1) and acute brainstem slices (Fig. 4; Gourine et al., 2010). Simultaneous imaging of changes in [Ca²⁺]_i and [Na⁺]_i in individual astrocytes recorded in organotypic brainstem slices demonstrated that acidification-induced Ca²⁺ responses in chemosensitive cells are accompanied by Na⁺ entry (*n* = 39 cells; *n* = 5 slices; Fig. 1a). [Ca²⁺]_i transients were not observed in brainstem astrocytes that were not responding to the decrease in pH with Na⁺ influx (*n* = 56 cells; *n* = 5 slices; Fig. 1b), suggesting that the mechanisms responsible for the increases in intracellular concentrations of both cations are coupled. Acidification-induced elevations in [Ca²⁺]_i in pH-sensitive astrocytes were reversibly abolished (*p* < 0.001, *F*_(1,113) = 1298) in Na⁺-free medium (replacement of Na⁺ with equimolar concen-

tration of choline; $n = 74$ cells; $n = 9$ slices; Fig. 1c), suggesting that Na⁺ entry triggers Ca²⁺ responses.

Acidic stimuli activate several parallel Na⁺-dependent mechanisms responsible for intracellular pH regulation, including Na⁺/H⁺ exchange and Na⁺/HCO₃⁻ cotransport (Shrode and Putnam, 1994). It was noted that astrocytes display elevations in [Ca²⁺]_i when aCSF is replaced with a Na⁺-free medium (Fig. 1c) and that in response to acidification, Na⁺ entry precedes Ca²⁺ responses (by 12.7 ± 0.9 s, $n = 19$ slices; Fig. 2a). This suggested that acidification-induced Ca²⁺ responses in astrocytes might be driven by elevations in [Na⁺]_i and reversal of NCX. Activation of either NHE, NBC, or both might be responsible for the increases in [Na⁺]_i in response to decreased pH. Acidification-induced [Ca²⁺]_i and [Na⁺]_i responses in astrocytes were not affected by the NHE inhibitor cariporide (10 μM, $n = 39$ cells; $n = 7$ slices; Fig. 2e,f). However, Na⁺ entry induced by a decrease in pH was abolished and Ca²⁺ responses were markedly reduced in the presence of NBC inhibitor S0859 (10 μM; $n = 32$ cells; $n = 6$ slices; $p < 0.001$, $F_{(1,71)} = 2540$; Fig. 2b,f) or anion exchange inhibitor DIDS (10 μM; which also interferes with NBC; $n = 18$ cells; $n = 3$ slices; $p < 0.001$, $F_{(1,36)} = 484$; Fig. 2f). NCX inhibitor SN-6 (10 μM) reduced ($n = 27$ cells; $n = 3$ slices; $p < 0.001$, $F_{(1,66)} = 540$; Fig. 2c,f), while combined NBC/NCX blockade [S0859 (10 μM)/SN-6 (10 μM)] reversibly abolished, astroglial [Na⁺]_i and [Ca²⁺]_i responses triggered by acidification ($n = 41$ cells; $n = 6$ slices; $p < 0.001$, $F_{(1,80)} = 9722$; Fig. 2d,f).

In a separate experiment, absolute level of resting and peak acidification-induced increases in [Na⁺]_i were determined (Fig. 3). There was no difference in resting level of [Na⁺]_i between pH-sensitive and pH-insensitive astrocytes recorded in organotypic slices (11.8 ± 0.2 mM, $n = 84$ cells, 4 slices vs 12.1 ± 0.1 mM, $n = 93$, 3 slices, respectively; $p = 0.28$). In chemosensitive astrocytes, [Na⁺]_i peaked at 19.7 ± 0.6 mM ($n = 84$, 4 slices) in response to acidification (Fig. 3c).

Chemosensory [Ca²⁺]_i responses recorded in ventral brainstem astrocytes expressing Ca²⁺ indicator *Case12* in acute slices of adult rats were reduced by S0859 ($n = 53$ cells; $n = 5$ slices), DIDS ($n = 27$ cells; $n = 5$ slices), and SN-6 ($n = 25$ cells; $n = 3$ slices), and were not affected by NHE blockade by amiloride (0.5 mM; $n = 16$ cells; $n = 3$ slices; $p > 0.05$) or inhibition of phospholipase C with U73122 (10 μM; $n = 37$ cells; $n = 4$ slices; $p > 0.05$; Fig. 4a,c). Astroglial [Ca²⁺]_i responses triggered by acidification in acute slices of the rat brainstem were reversibly

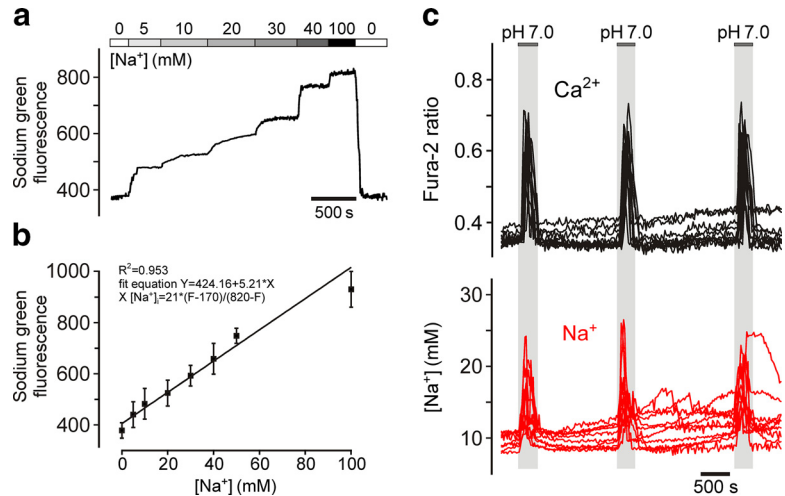


Figure 3. Estimation of absolute resting level and peak acidification-induced increases in [Na⁺]_i in chemosensitive brainstem astrocytes. **a**, Calibration of Na⁺-sensitive fluorescence signal in astrocytes of organotypic brainstem slices recorded in the presence of gramicidin D, monensin, and ouabaine (to equilibrate Na⁺ across the cell membrane) at increasing extracellular [Na⁺]. Averaged trace of Sodium Green fluorescence changes in 152 astrocytes recorded in three organotypic brainstem slices is shown. **b**, Sodium Green fluorescence plotted as a function of [Na⁺]. **c**, Representative example illustrating the resting level and peak acidification-induced increases in [Na⁺]_i in chemosensitive brainstem astrocytes. Traces depict responses of 10 individual cells recorded in an organotypic brainstem slice preparation.

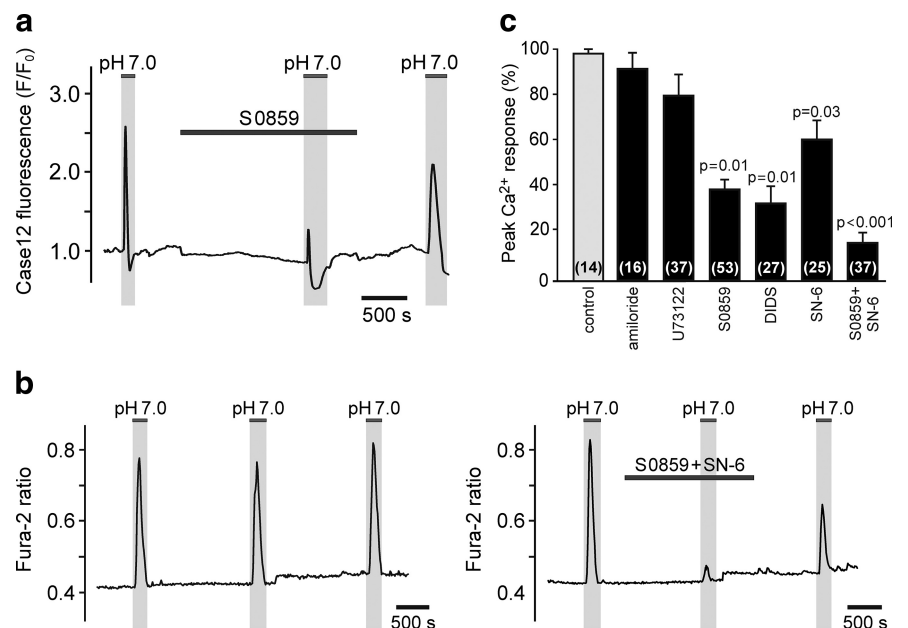


Figure 4. Pharmacology of acidification-induced [Ca²⁺]_i responses in astrocytes recorded in acute slices of the rat brainstem. **a**, Representative recording illustrating the effect of NBC blockade (S0859, 30 μM) on [Ca²⁺]_i responses in brainstem astrocytes induced by decreases in pH. Averaged traces of [Ca²⁺]_i changes in 14 astrocytes transfected to express Ca²⁺ indicator *Case12* and recorded in an acute horizontal brainstem slice are shown. **b**, Representative recordings illustrating acidification-induced [Ca²⁺]_i responses of brainstem astrocytes in control conditions and in conditions of combined NBC/NCX blockade [S0859 (10 μM)/SN-6 (10 μM)]. Averaged traces of [Ca²⁺]_i changes in 14 (left) and 15 (right) astrocytes recorded in separate experiments in acute horizontal slices of the rat brainstem are shown. **c**, Summary data (expressed as the percentage of the initial response) of the pharmacology of acidification-induced Ca²⁺ responses in astrocytes recorded in acute brainstem slices.

reduced by 86% in conditions of combined NBC/NCX blockade [S0859 (10 μM)/SN-6 (10 μM); $n = 37$ cells; $n = 4$ slices; $p < 0.001$, $F_{(1,51)} = 177$; Fig. 4b,c].

To identify the transporter(s) responsible for the high sensitivity of brainstem astrocytes to decreases in pH, brainstem and cortical (not sensitive to changes in pH; Kasymov et al., 2013) astrocytes were isolated and differences in the expression of genes

Table 1. NBC, NHE, and inwardly rectifying K⁺ channel gene expression differences between cortical and brainstem astrocytes

	Culture			Neonate			Adult		
	Brainstem	Cortex	Fold difference	Brainstem	Cortex	Fold difference	Brainstem	Cortex	Fold difference
NBCs									
SLC4a4	53.3	13.4	4.0	836.9	140.2	6.0	421.1	18.3	23.0
SLC4a5	4.5	0	—	1.8	4.5	0.4	5.1	0.4	12.8
SLC4a7	9.5	14.0	0.7	8.2	16.4	0.5	7.4	24.0	0.3
SLC4a8	0	0	—	0	0	—	0	0	—
SLC4a9	0	0	—	0	0	—	0	0	—
SLC4a10	3.3	0	—	11.2	2.4	4.7	2.0	5.6	0.4
SLC4a11	0	0	—	0	0	—	0	0	—
NHEs									
SLC9A1	13.2	18.6	0.7	28.0	39.9	0.7	20.8	39.2	0.5
SLC9A2	0	0	—	0.5	0	—	0	1.9	—
SLC9A3	0.3	0	—	0	0.1	—	0	0	—
SLC9A4	0	0	—	0	0	—	0	0	—
SLC9A5	2.0	1.3	1.5	1.2	3.5	0.3	0.3	0	—
SLC9B1	0	0	—	0	0	—	0	0	—
Inwardly rectifying K⁺ channels									
KCNJ10	127.9	19.0	6.7	188.4	100.5	1.9	709.9	23.1	30.7
KCNJ16	0.4	0.7	0.6	55.9	1.1	50.8	92.5	6.2	14.9

Data are presented in fragments per kilobase of transcript sequence per million mapped fragments.

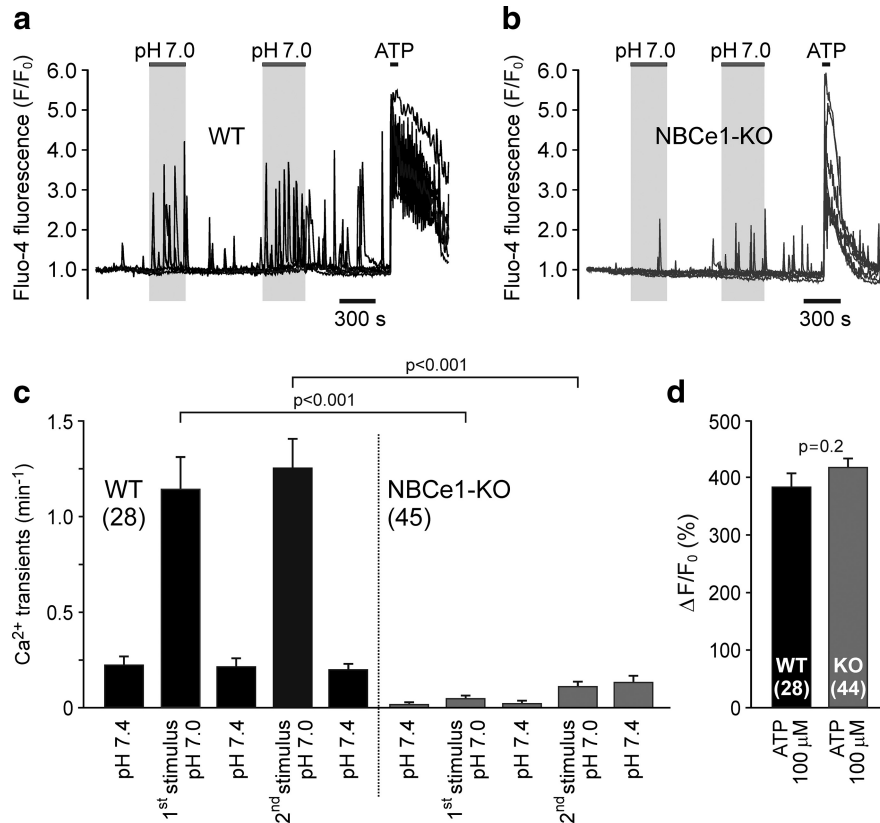


Figure 5. NBCe1 activity is responsible for acidification-induced [Ca²⁺]_i responses in chemosensitive brainstem astrocytes. **a**, **b**, Representative examples of [Ca²⁺]_i responses to CO₂-induced acidification (decreases in pH from 7.4 to 7.0 induced by an increase in [CO₂] from 2 to 5% in aCSF containing 10 mM HCO₃⁻) in cultured brainstem astrocytes of wild-type (WT) and *NBCe1* knock-out (*NBCe1*-KO) mice. Each plot illustrates responses of six individual astrocytes. **c**, Summary data illustrating frequency of fast Ca²⁺ oscillations recorded in cultured astrocytes of WT and *NBCe1*-KO mice at resting conditions, pH 7.4, and during two chemosensory challenges, pH 7.0. **d**, Summary data illustrating peak amplitudes of [Ca²⁺]_i responses induced by application of ATP in cultured astrocytes of WT and *NBCe1*-KO mice.

tions/developmental stages: in cultured astrocytes, in astrocytes acutely isolated from the brains of neonatal (P3) rats, and in astrocytes acutely isolated from the brains of young adult rats (Table 1). Brainstem astrocytes also showed higher expression of another notable astroglial gene, *KCNJ10* (Table 1), which encodes the Kir4.1 subunit of inwardly rectifying K⁺ channels (potential significance of high Kir4.1 expression for astroglial chemosensitivity is discussed below).

These transcriptome data suggested that different levels of NBCe1 expression may underlie regional differences in pH sensitivity between astrocytes and that NBCe1 is the key transporter responsible for acidification-induced Na⁺ entry and Ca²⁺ responses in chemosensitive astrocytes. To test this hypothesis, [Ca²⁺]_i responses induced by decreases in pH were next assessed in brainstem astrocytes of *NBCe1*-deficient mice. Cultured brainstem astrocytes of wild-type mice responded to CO₂-induced acidification with increased rate of fast Ca²⁺ oscillations (*n* = 28 cells, *n* = 2 cultures; Fig. 5*a,c*; Kasymov et al., 2013). These acidification-induced [Ca²⁺]_i responses were markedly reduced in conditions of *NBCe1* deficiency (*n* = 45 cells, *n* = 4 cultures; *p* < 0.001, *F*_(1,292) = 81; Fig. 5*b,c*). Amplitudes of [Ca²⁺]_i elevations induced by ATP (100 μM) were similar in cultured astrocytes of wild-type and *NBCe1* knock-out mice (Fig. 5*a,b,d*), indicating that reduced frequency of pH-evoked [Ca²⁺]_i oscillations is not due to the effect of *NBCe1* deficiency on cellular Ca²⁺ recruitment/handling mechanisms.

encoding all known NBCs and NHEs were analyzed (Table 1). Only the expression of *SLC4a4* gene encoding electrogenic Na⁺/HCO₃⁻ cotransporter NBCe1 was found to be consistently higher in the brainstem (vs cortex) across different experimental condi-

Discussion

Intracellular Ca²⁺ governs key functions of astrocytes, including gliotransmitter release (Araque et al., 2014), lactate pro-

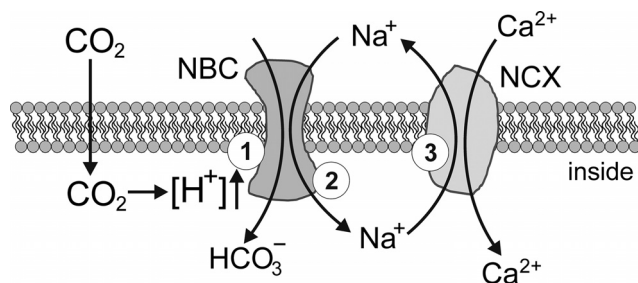


Figure 6. Plausible membrane mechanisms underlying chemosensory [Ca²⁺]_i responses in astrocytes induced by increases in P_{CO₂}/[H⁺]. CO₂-induced intracellular acidification triggers activation of NBC (1), which brings Na⁺ inside the cell (2). Raising [Na⁺]_i activates NCX to operate in a reverse mode (3), leading to Ca²⁺ entry.

duction (Tang et al., 2014), and control of cerebral vasculature (Attwell et al., 2010). Physiological decreases in pH trigger [Ca²⁺]_i responses in specialized pH-sensitive astrocytes that populate the ventral regions of the brainstem (Gourine et al., 2010; Kasymov et al., 2013; Turovsky et al., 2015). Results of the present study suggest that in pH-sensitive astrocytes, acidification activates NBCe1, which brings Na⁺ inside the cell. Raising [Na⁺]_i activates NCX to operate in a reverse mode, leading to Ca²⁺ entry (Fig. 6) followed by activation of the downstream signaling pathways.

Several previous studies addressed the potential mechanisms underlying the sensitivity of brainstem astrocytes to changes in pH (Gourine et al., 2010; Wenker et al., 2010, 2012; Kasymov et al., 2013). Recordings of changes in membrane potential of brainstem astrocytes in acute slices of neonatal rats demonstrated moderate depolarizations (by 4–9 mV) in response to acidification (in HEPES-buffered solution from pH 7.5 to 6.9 or in aCSF saturated with 10–15% CO₂, pH 6.8–7.1; Ritucci et al., 2005; Wenker et al., 2010). The pharmacological profile of the CO₂/H⁺-sensitive current in ventral brainstem astrocytes suggested involvement of inward rectifying potassium channels (like Kir4.1/Kir5.1) and certain DIDS-sensitive NBCs (Wenker et al., 2010). These results, however, did not provide an answer on how changes in intracellular or extracellular P_{CO₂}/[H⁺] trigger Ca²⁺ responses, since astrocytes *in situ* do not express voltage-operated Ca²⁺ channels (Carmignoto et al., 1998). Indeed, in brainstem astrocytes, depolarization by >20 mV by current injections failed to trigger [Ca²⁺]_i responses in the recorded and neighboring astrocytes (Gourine et al., 2010). The same study reported that acidification-induced Ca²⁺ responses in brainstem astrocytes are not affected in the presence of various pharmacological agents that interfere with several potential targets, including pH-sensitive K⁺, TRPV, and TRPP channels (Gourine et al., 2010).

There is evidence that brainstem astrocytes possess mechanism(s) of direct (i.e., independent of changes in [H⁺], [HCO₃⁻], and [Ca²⁺]_i) CO₂ sensing (Huckstepp et al., 2010) that operates via modulation of the connexin-26 hemichannel opening (Meigh et al., 2013), leading to CO₂-dependent release of ATP (Huckstepp et al., 2010). This mechanism appears to be independent of, and does not contribute to, astroglial pH sensing, since acidification-induced Ca²⁺ responses in brainstem astrocytes are either not affected or only partially reduced by pharmacological agents that block functional connexin/pannexin hemichannels (Gourine et al., 2010).

Hirata and Oku (2010) reported that acidification (pH 7.1)-induced Ca²⁺ responses in glia-rich brainstem cultures are not observed in HCO₃⁻-free HEPES-buffered medium. The current study was further motivated by the data reported recently that suggested that NBCe1 expressed in astrocytes is a high-affinity HCO₃⁻ carrier capable of fast and effective cytosolic H⁺ buffering (Theparambil et al., 2014; Theparambil and Deitmer, 2015). This NBC is rapidly activated in response to acidic stimuli and requires only micromolar extracellular [HCO₃⁻]_o to operate (Theparambil et al., 2014). We hypothesized that NBC activation by decreased pH_i leading to rapid HCO₃⁻ and Na⁺ entry may trigger Ca²⁺ responses by activation of NCX to operate in a reverse mode (Rojas et al., 2007; Kirischuk et al., 2012; Parpura and Verkhratsky, 2012). The data obtained in the present study showing that acidification-induced [Ca²⁺]_i responses in astrocytes are preceded by Na⁺ entry, significantly reduced by NBC blockade and abolished in Na⁺-free medium or in conditions of NBCe1 deficiency, provide strong supporting evidence of the key role played by Na⁺/HCO₃⁻ cotransport in the mechanisms underlying pH sensitivity of brainstem astrocytes. Reversal of NCX following Na⁺ entry appears to be responsible for subsequent increases in [Ca²⁺]_i. This conclusion is supported by the results of electrophysiological studies that demonstrated that the membrane potential of pH-responsive brainstem astrocytes in HCO₃⁻-buffered medium is between –75 and –82 mV (Wenker et al., 2010), which is very close to the calculated reversal potential of NCX (–80 mV; Kirischuk et al., 2012) set by a relatively high (15–20 mM) [Na⁺]_i in astrocytes (Kirischuk et al., 2012; Parpura and Verkhratsky, 2012). Indeed, in pH-sensitive brainstem astrocytes, the resting [Na⁺]_i was found to be ~12 mM, increasing to ~20 mM during the chemosensory challenge.

Ventral regions of the brainstem are populated by functionally specialized astrocytes, which are different (in terms of their high pH-sensitivity) from the majority of astroglia residing in other parts of the CNS (Kasymov et al., 2013). What makes some astrocytes chemosensitive, i.e., capable of mounting Ca²⁺ responses to changes in pH? Higher expression of certain membrane channels, which maintain membrane potential at an appropriate level for NCX reversal, may determine astroglial pH sensitivity. Inwardly rectifying K⁺ channels containing the Kir4.1 subunit are believed to be largely responsible for establishing the resting membrane potential in astrocytes (Olsen and Sontheimer, 2008). Comparative analysis of brainstem and cortical astroglial transcriptomes performed in this study revealed higher expression of the Kir4.1 subunit in chemosensitive astrocytes. Interestingly, in mice, conditional deletion of the Kir4.1 subunit in astrocytes dramatically reduces central respiratory CO₂ chemosensitivity (Hawkins et al., 2014), suggesting that in conditions of an established deletion of the key astroglial membrane channel, brainstem astrocytes are not able to sense changes in pH. It appears, however, that the differences between pH-sensitive and pH-insensitive astrocytes lay upstream from NCX reversal. Indeed, the results of this study showed that acidification-induced [Ca²⁺]_i responses are triggered by Na⁺ entry, which is not observed in pH-insensitive astrocytes (although the resting [Na⁺]_i was found to be similar in two astroglial populations). Therefore, we next hypothesized that differential expression and activities of certain NBCs underlie differences in pH-sensitivity between astrocytes.

Transcriptome analysis identified astroglial NBCe1 expression to be consistently higher in the brainstem (vs cortex) across different experimental conditions/developmental stages, suggesting that NBCe1 is the transporter responsible for acidification-induced Na⁺ entry and Ca²⁺ responses in chemosensitive astrocytes. Indeed,

[Ca²⁺]_i responses induced by decreases in pH were found to be markedly reduced in brainstem astrocytes of *NBCe1*-deficient mice. *NBCe1* is critically important for homeostasis as these knock-out animals do not survive beyond the third week of life. They display profound metabolic acidosis (Gawenis et al., 2007) and breathing deficit may contribute to this harmful phenotype. An extension of this study would require development of a novel transgenic mouse line allowing assessment of the respiratory activity following selective conditional deletion of *NBCe1* in (brainstem) astrocytes.

Current models of central respiratory CO₂ chemosensitivity (i.e., mechanisms that detect changes in brainstem parenchymal P_{CO₂}/[H⁺] and trigger adaptive changes in ventilation) are centered at a group of specialized pH-sensitive neurons of the retrotrapezoid nucleus located near the ventral surface of the medulla oblongata (Guyenet, 2014). These chemosensitive neurons are proposed to play the key role, with neighboring pH-sensitive astrocytes providing an additional 20–30% of the chemosensory drive to breathe (Guyenet, 2014). However, there is evidence that the sensitivity of retrotrapezoid nucleus neurons to decreases in pH is, to a large extent, mediated by prior release of gliotransmitters(s), primarily ATP (Gourine et al., 2010). In addition, increases in ventilation are triggered when pH-evoked [Ca²⁺]_i responses in ventral brainstem astrocytes are mimicked by optogenetic stimulation (Gourine et al., 2010), while in mice astrocyte-specific conditional deletion of certain genes (*MeCP2*, *Kir4.1*) is sufficient to dramatically impair ventilatory CO₂ chemosensitivity (Hawkins et al., 2014; Garg et al., 2015). It appears, therefore, that intact pH-sensitive retrotrapezoid nucleus neurons (Guyenet, 2014) are not able to mount an appropriate ventilatory response when astroglial function and pH sensitivity are compromised. Together these lines of evidence support the idea of an important role played by astroglial pH sensitivity in the brain mechanisms linking changes in brainstem parenchymal P_{CO₂}/[H⁺] and central respiratory drive. The data obtained in the present study suggest that *NBCe1* and *NCX* activities underlie functional CO₂/H⁺ sensitivity of brainstem astrocytes that contribute to homeostatic regulation of brain parenchymal pH and control of breathing.

References

- Angelova PR, Kasymov V, Christie I, Sheikhbaehaei S, Turovsky E, Marina N, Korsak A, Zwicker J, Teschemacher AG, Ackland GL, Funk GD, Kasparov S, Abramov AY, Gourine AV (2015) Functional oxygen sensitivity of astrocytes. *J Neurosci* 35:10460–10473. [CrossRef Medline](#)
- Araque A, Carmignoto G, Haydon PG, Oliet SH, Robitaille R, Volterra A (2014) Gliotransmitters travel in time and space. *Neuron* 81:728–739. [CrossRef Medline](#)
- Attwell D, Buchan AM, Charpak S, Lauritzen M, Macvicar BA, Newman EA (2010) Glial and neuronal control of brain blood flow. *Nature* 468:232–243. [CrossRef Medline](#)
- Carmignoto G, Pasti L, Pozzan T (1998) On the role of voltage-dependent calcium channels in calcium signaling of astrocytes *in situ*. *J Neurosci* 18:4637–4645. [Medline](#)
- Ch'en FF, Villafuente FC, Swietach P, Cobden PM, Vaughan-Jones RD (2008) S0859, an N-cyanosulphonamide inhibitor of sodium-bicarbonate cotransport in the heart. *Br J Pharmacol* 153:972–982. [CrossRef Medline](#)
- Garg SK, Liou DT, Knopp SJ, Bissonnette JM (2015) Conditional depletion of methyl-CpG-binding protein 2 in astrocytes depresses the hypercapnic ventilatory response in mice. *J Appl Physiol* 119:670–676. [CrossRef Medline](#)
- Gawenis LR, Bradford EM, Prasad V, Lorenz JN, Simpson JE, Clarke LL, Woo AL, Grisham C, Sanford LP, Doetschman T, Miller ML, Shull GE (2007) Colonic anion secretory defects and metabolic acidosis in mice lacking the NBC1 Na⁺/HCO₃⁻ cotransporter. *J Biol Chem* 282:9042–9052. [CrossRef Medline](#)
- Gourine AV, Llaudet E, Dale N, Spyer KM (2005) ATP is a mediator of chemosensory transduction in the central nervous system. *Nature* 436:108–111. [CrossRef Medline](#)
- Gourine AV, Kasymov V, Marina N, Tang F, Figueiredo MF, Lane S, Teschemacher AG, Spyer KM, Deisseroth K, Kasparov S (2010) Astrocytes control breathing through pH-dependent release of ATP. *Science* 329:571–575. [CrossRef Medline](#)
- Guo F, Liu B, Tang F, Lane S, Souslova EA, Chudakov DM, Paton JF, Kasparov S (2010) Astroglia are a possible cellular substrate of angiotensin(1–7) effects in the rostral ventrolateral medulla. *Cardiovasc Res* 87:578–584. [CrossRef Medline](#)
- Guyenet PG (2014) Regulation of breathing and autonomic outflows by chemoreceptors. *Compr Physiol* 4:1511–1562. [CrossRef Medline](#)
- Halassa MM, Haydon PG (2010) Integrated brain circuits: astrocytic networks modulate neuronal activity and behavior. *Annu Rev Physiol* 72:335–355. [CrossRef Medline](#)
- Hawkins V, Kuo F, Bellemare L, Perez D, Dubreuil T, Mulkey D (2014) Conditional knockdown of Kir4.1 in astrocytes blunts the hypercapnic respiratory response in awake mice. *FASEB J* 28:872.7. [CrossRef](#)
- Haydon PG, Carmignoto G (2006) Astrocyte control of synaptic transmission and neurovascular coupling. *Physiol Rev* 86:1009–1031. [CrossRef Medline](#)
- Henneberger C, Papouin T, Oliet SH, Rusakov DA (2010) Long-term potentiation depends on release of D-serine from astrocytes. *Nature* 463:232–236. [CrossRef Medline](#)
- Hirata Y, Oku Y (2010) TRP channels are involved in mediating hypercapnic Ca²⁺ responses in rat glia-rich medullary cultures independent of extracellular pH. *Cell Calcium* 48:124–132. [CrossRef Medline](#)
- Huckstepp RT, Id Bihi R, Eason R, Spyer KM, Dicke N, Willecke K, Marina N, Gourine AV, Dale N (2010) Connexin hemichannel-mediated CO₂-dependent release of ATP in the medulla oblongata contributes to central respiratory chemosensitivity. *J Physiol* 588:3901–3920. [CrossRef Medline](#)
- Kasymov V, Larina O, Castaldo C, Marina N, Patrushev M, Kasparov S, Gourine AV (2013) Differential sensitivity of brainstem versus cortical astrocytes to changes in pH reveals functional regional specialization of astroglia. *J Neurosci* 33:435–441. [CrossRef Medline](#)
- Kirischuk S, Parpura V, Verkhratsky A (2012) Sodium dynamics: another key to astroglial excitability? *Trends Neurosci* 35:497–506. [CrossRef Medline](#)
- Liou DT, Garg SK, Monaghan CE, Raber J, Foust KD, Kaspar BK, Hirrlinger PG, Kirchhoff F, Bissonnette JM, Ballas N, Mandel G (2011) A role for glia in the progression of Rett's syndrome. *Nature* 475:497–500. [CrossRef Medline](#)
- Magistretti PJ (2006) Neuron-glia metabolic coupling and plasticity. *J Exp Biol* 209:2304–2311. [CrossRef Medline](#)
- Meigh L, Greenhalgh SA, Rodgers TL, Cann MJ, Roper DI, Dale N (2013) CO₂ directly modulates connexin26 by formation of carbamate bridges between subunits. *Elife* 2:e01213. [CrossRef Medline](#)
- Olsen ML, Sontheimer H (2008) Functional implications for Kir4.1 channels in glial biology: from K⁺ buffering to cell differentiation. *J Neurochem* 107:589–601. [CrossRef Medline](#)
- Parpura V, Verkhratsky A (2012) Homeostatic function of astrocytes: Ca²⁺ and Na⁺ signalling. *Transl Neurosci* 3:334–344. [Medline](#)
- Ritucci NA, Erlichman JS, Leiter JC, Putnam RW (2005) Response of membrane potential and intracellular pH to hypercapnia in neurons and astrocytes from rat retrotrapezoid nucleus. *Am J Physiol Regul Integr Comp Physiol* 289:R851–R861. [Medline](#)
- Rojas H, Colina C, Ramos M, Benaim G, Jaffe EH, Caputo C, DiPolo R (2007) Na⁺ entry via glutamate transporter activates the reverse Na⁺/Ca²⁺ exchange and triggers Ca²⁺_i-induced Ca²⁺ release in rat cerebellar Type-1 astrocytes. *J Neurochem* 100:1188–1202. [CrossRef Medline](#)
- Shrode LD, Putnam RW (1994) Intracellular pH regulation in primary rat astrocytes and C6 glioma cells. *Glia* 12:196–210. [CrossRef Medline](#)
- Tang F, Lane S, Korsak A, Paton JF, Gourine AV, Kasparov S, Teschemacher AG (2014) Lactate-mediated glia-neuronal signalling in the mammalian brain. *Nat Commun* 5:3284. [CrossRef Medline](#)
- Theparambil SM, Deitmer JW (2015) High effective cytosolic H⁺ buffering

- in mouse cortical astrocytes attributable to fast bicarbonate transport. *Glia* 63:1581–1594. [CrossRef Medline](#)
- Theparambil SM, Ruminot I, Schneider HP, Shull GE, Deitmer JW (2014) The electrogenic sodium bicarbonate cotransporter NBCe1 is a high-affinity bicarbonate carrier in cortical astrocytes. *J Neurosci* 34:1148–1157. [CrossRef Medline](#)
- Turovsky E, Karagiannis A, Abdala AP, Gourine AV (2015) Impaired CO₂ sensitivity of astrocytes in a mouse model of Rett syndrome. *J Physiol* 593:3159–3168. [CrossRef Medline](#)
- Volterra A, Meldolesi J (2005) Astrocytes, from brain glue to communication elements: the revolution continues. *Nat Rev Neurosci* 6:626–640. [CrossRef Medline](#)
- Wenker IC, Kréneisz O, Nishiyama A, Mulkey DK (2010) Astrocytes in the retrotrapezoid nucleus sense H⁺ by inhibition of a Kir4.1/5.1-like current and may contribute to chemoreception by a purinergic mechanism. *J Neurophysiol* 104:3042–3052. [CrossRef Medline](#)
- Wenker IC, Sobrinho CR, Takakura AC, Moreira TS, Mulkey DK (2012) Regulation of ventral surface CO₂/H⁺-sensitive neurons by purinergic signaling. *J Physiol* 590:2137–2150. [CrossRef Medline](#)
- Zhang Y, Chen K, Sloan SA, Bennett ML, Scholze AR, O’Keefe S, Phatnani HP, Guarnieri P, Caneda C, Ruderisch N, Deng S, Liddelow SA, Zhang C, Daneman R, Maniatis T, Barres BA, Wu JQ (2014) An RNA-sequencing transcriptome and splicing database of glia, neurons, and vascular cells of the cerebral cortex. *J Neurosci* 34:11929–11947. [CrossRef Medline](#)